Electronic Supporting Information

Turn-on type afterglow probe for Hg^{2+} sensing by a PVA-mediated triplet sensitizer

Satoshi Takegawa, Masato Ito and Yuji Kubo*

Department of Applied Chemistry, Graduate School of Urban Environmental Sciences, Tokyo Metropolitan University, 1-1 Minami-Osawa, Hachioji, Tokyo, 192-0397

Table of contents

Experimental Section

General

NMR spectra were measured on a Bruker Advance 500 spectrometer (^{1}H: 500 MHz, ^{13}C: 126 MHz) or JEOL JNM-ESC400 (^{1}H: 400 MHz, ^{13}C; 101 MHz). In ^{1}H and ^{13}C NMR measurements, chemical shifts (δ) are reported downfield from the internal standard Me_4Si and $BF_3{\cdot}OEt_2$, respectively. The absorption and emission were measured using Shimadzu UV-3600 UV/vis spectroscopy and a JASCO FP-8500 spectrofluorometer, respectively. FT-IR spectra were recorded on a JASCO FT/IR-4100 spectrometer with NaCl salt plate. The absolute photoluminescence quantum yields (Φ) for emission up to 650 nm were determined by JASCO FP-8500 spectrofluorometer equipped integral sphere (ϕ = 60 mm). Photographic images were taken with digital camera (Canon, EOS Kiss X8i).

Materials

Unless otherwise indicated, reagents used for the synthesis were commercially available and were used as supplied. Bis[4-(4,4,5,5-tetramethyl-1,3,2-dioxaborolan-2-yl)phenyl]methanone[1] and 2-methoxy-9*H*-thioxanthen-9-one **2**[2] were prepared according to method previously reported.

Bis[4-dihydroxyborylphenyl]methanone BPBA

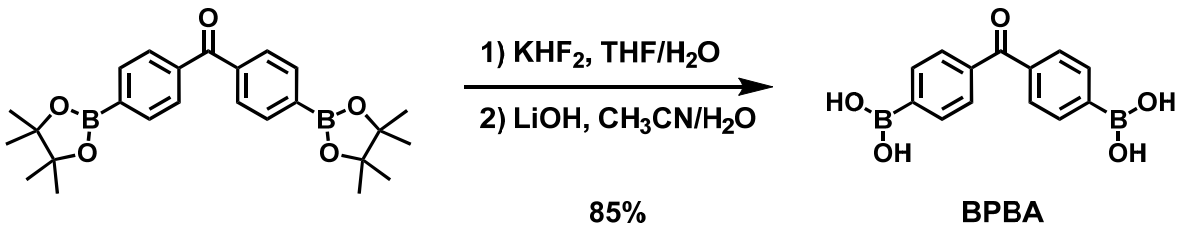

Scheme 1. Synthesis route of **BPBA.**

To a solution of bis[4-(4,4,5,5-tetramethyl-1,3,2-dioxaborolan-2-yl)phenyl]methanone (0.262 g, 0.60 mmol) in THF (10 mL) was added 3.0 M KHF_2 aqueous solution (1.0 mL). The resultant solution was stirred for 3 h at room temperature. After adding CH_3OH and H_2O, the solution was evaporated to remove pinacol as side product. The solid was extracted with CH_3CN to obtain the intermediate, being dissolved in CH_3CN (8 mL) and H_2O (9 mL). To the solution was added an aqueous solution of 1.0 M LiOH (6.0 mL) for 22 h. After neutralization with 1M HCl, the solution was extracted with CH_3CN for three times. The organic layer was evaporated to obtain white solid in 85% yield. ^{1}H NMR (400 MHz, DMSO-d_6): δ (ppm), 8.32 (s, 4H), 7.94 (d, J = 8.0 Hz, 4H), 7.68 (d, J = 8.0 Hz). ^{13}C NMR (101 MHz, DMSO-d_6): δ (ppm), 196.4, 138.2, 134.1, 128.5. The signals arising from the carbon atoms bound to the boron one were undetectable due to the quadrupolar relaxation. HRMS (FAB): calcd for $C_{19}H_{21}B_2O_7$ $[M(Glycerol)_2+H]^+$: 383.1468, found 383.1469. Glycerol was used as a matrix.

2-Methoxy-9*H*- thioxanthene-9-thione 1

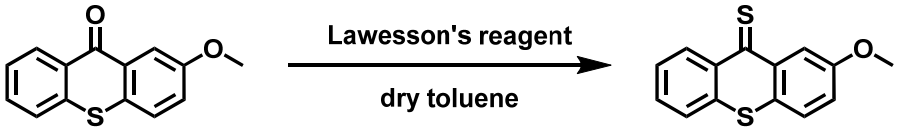

2 quant 1

Scheme 2. Synthesis route of **1.**

2-Methoxy-thioxanthen-9-one **2** (0.314 g, 1.3 mmol) and Lawesson's reagent (1.13 g, 2.8 mmol) were dissolved in toluene (10 mL) under N_2 atmosphere. The resultant solution was refluxed at 80 ºC for 3 h. After quenching the reaction by water, the solution was extracted with AcOEt for three times. And the organic phase was then dried with Na_2SO_4, evaporated in vacuo and chromatographed on silica gel (Wacogel C-300) using CH_2Cl_2/hexane (1:1 v/v). In this way, 0.339 g of **1** was obtained quantitatively. ^{1}H NMR (500 MHz, $CDCl_3$): δ (ppm), 9.08 (d, J = 8.5 Hz, 1H), 8.59 (d, J = 2.8 Hz 1H), 7.61 (d, J = 3.7 Hz, 2H), 7.53 (d, J = 8.8, 1H), 7.46 (dt, J =8.4, 4.2 Hz, 1H), 7.30 (dd, J =8.8, 2.8 Hz, 1H), 3.96 (s, 3H). ^{13}C NMR (126 MHz, DMSO-d_6): δ (ppm), 207.7, 158.9, 137.4, 135.8, 133.1, 132.3, 131.9, 128.3, 127.5, 126.7, 124.0, 122.5, 114.0, 55.5. FAB-MS: m/z = 259 $[M+H]^+$. Elemental analysis for $C_{14}H_{10}OS_2$: C 65.09, H 3.90, N 0, Found: C 65.05, H 3.92.

Fabrication of benzoylphenyl boronate-crosslinked PVA film (BPB@PVA)

The film was fabricated by drop-casting DMSO solution (500 μL) of commercial PVA (number average molecular weight (M_n) of 89000 – 98000; saponification number = 99%, 0.40 unit M[3]) and **BPBA** (8.0 mM), followed by solvent exchange with water and dried in vacuo. The resultant films were characterized by FT-IR cm^{-1}) ; 3336, 2942, 1652, 1418, 1306, 1094, 931, 853, 699, 672, 642.

Fabrication of 2-doped BPB@PVA (2/BPB@PVA)

The film was fabricated by drop-casting DMSO solution (500 μL) of commercial PVA (number average molecular weight (M_n) of 89000 – 98000; saponification number = 99%, 0.40 unit M[3]), **BPBA** (8.0 mM) and **2** (0.40 mM), followed by solvent exchange with water and dried in vacuo.

Fabrication of 1-doped BPB@PVA (1/BPB@PVA)

The film was fabricated by drop-casting DMSO solution (500 μL) of commercial PVA (number average molecular weight (M_n) of 89000 – 98000; saponification number = 99%, 0.40 unit M[3]), **BPBA** (8.0 mM) and **1** (0.40 mM), followed by solvent exchange with water and dried in vacuo.

References

1. X. Miao, Z. Cai, J. Li, L. Liu, J. Wu, B. Li, L. Ying, F. Silly, W. Deng and Y. Cao, *ChemPhotoChem*, 2021, **5**, 626-631.
2. M. Bhanuchandra, H. Yorimitsu and A. Osuka, *Org. Lett.*, 2016, **18**, 384-387.
3. The concentration was based on monomer unit.

DFT/TD-DFT calculation

Density functional theory (DFT) calculations at the ωB97X-D3/def2-TZVP level were performed in the Orca 4.2.1 software. These molecular orbitals were visualized using Gauss view 6.0.16 program. The molecular structures of **BPBA**, **1** and **2** optimized in the lowest singlet excited state are displayed below.

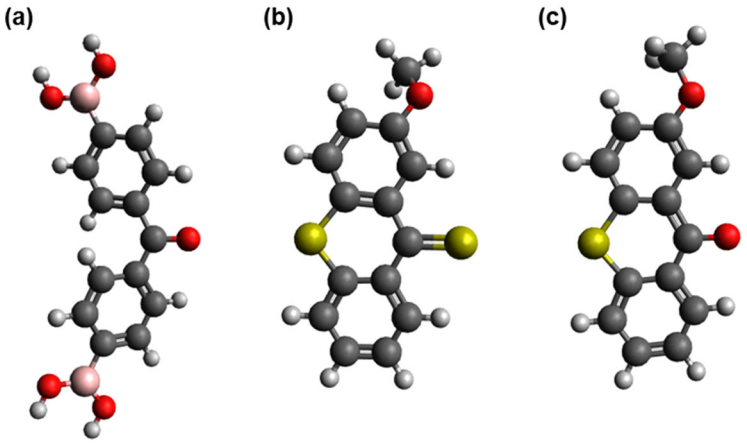

Table S1. Energy levels and electronic transition characters of **BPBA** optimized in the lowest singlet excited state. The frontier molecular orbitals of the dye are shown in Figure S1.

State	Energy	Oscillator strength	Transition
S_1	3.261 eV	0.0011	HOMO-4→LUMO (43.8%)
	(380 nm)		HOMO→LUMO (42.8%)
S_2	4.700 eV	0.0259	HOMO-2→LUMO (55.9%)
	(264 nm)		HOMO-4→LUMO (12.8%)
			HOMO-3→LUMO+1 (10.6%)
S_3	4.737 eV	0.1751	HOMO-3→LUMO (41.4%)
	(262 nm)		HOMO-1→LUMO (31.5%)
			HOMO-2→LUMO+1 (7.6%)
S_4	4.824 eV	0.5519	HOMO-1→LUMO (54.2%)
	(257 nm)		HOMO-3→LUMO (30.0%)
S_5	5.009 eV	0.1151	HOMO→LUMO (40.9%)
	(248 nm)		HOMO-4→LUMO (30.3%)
T_1	2.536 eV	0	HOMO→LUMO (76.4%)
	(489 nm)		HOMO-1→LUMO+1 (5.3%)
T_2	2.977 eV	0	HOMO-4→LUMO (65.3%)
	(417 nm)		HOMO-2→LUMO (10.6%)
			HOMO-1→LUMO+1 (5.7%)
			HOMO-4→LUMO+6 (5.2%)

T_3	3.242 eV (382 nm)	0	HOMO-1→LUMO (54.9%) HOMO→LUMO+1 (16.3%) HOMO-3→LUMO+3 (5.4%)
T_4	3.909 eV (317 nm)	0	HOMO-2→LUMO (60.4%) HOMO-3→LUMO+1 (22.2%)
T_5	3.949 eV (314 nm)	0	HOMO-3→LUMO (64.7%) HOMO-2→LUMO+1 (25.9%)

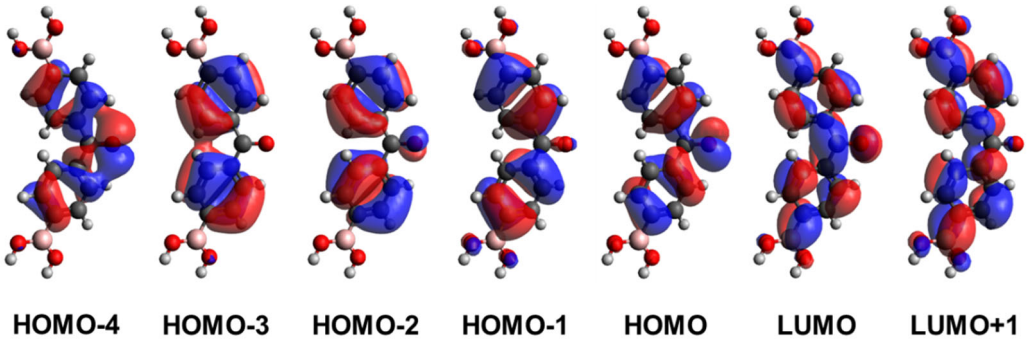

Figure S1. Molecular orbitals of **BPBA** calculated at ωB97X-D3/def2-TZVP level.

Table S2. Energy levels and electronic transition characters of **1** optimized in the lowest singlet excited state.

State	Energy	Oscillator strength	Transition
S_1	2.001 eV (620 nm)	0.0004	HOMO-1→LUMO (94.8%)
S_2	3.151 eV (393 nm)	0.1907	HOMO→LUMO (96.0%)
S_3	3.779 eV (328 nm)	0.0331	HOMO-2→LUMO (94.5%)
S_4	4.312 eV (288 nm)	0.0095	HOMO-3→LUMO (51.6%) HOMO→LUMO+1 (33.9%)
S_5	4.535 eV (273 nm)	0.0729	HOMO-4→LUMO (74.4%) HOMO-2→LUMO+1 (4.6%) HOMO-3→LUMO (4.6%)
S_6	4.920 eV (252 nm)	0.4982	HOMO→LUMO+1 (54.5%) HOMO-3→LUMO (20.9%) HOMO-4→LUMO (13.2%)
T_1	1.453 eV (854 nm)	0	HOMO→LUMO (60.7%) HOMO-2→LUMO (29.0%)
T_2	1.644 eV (754 nm)	0	HOMO-1→LUMO (92.3%)

T_3	2.777 eV (447 nm)	0	HOMO-2→LUMO (55.1%) HOMO→LUMO (32.0%)
T_4	3.180 eV (390 nm)	0	HOMO-4→LUMO (32.2%) HOMO→LUMO+1 (22.4%) HOMO-3→LUMO (13.4%) HOMO-2→LUMO+3 (6.6%)
T_5	3.656 eV (339 nm)	0	HOMO-3→LUMO (35.2%) HOMO-4→LUMO (22.9%) HOMO→LUMO+1 (15.7)

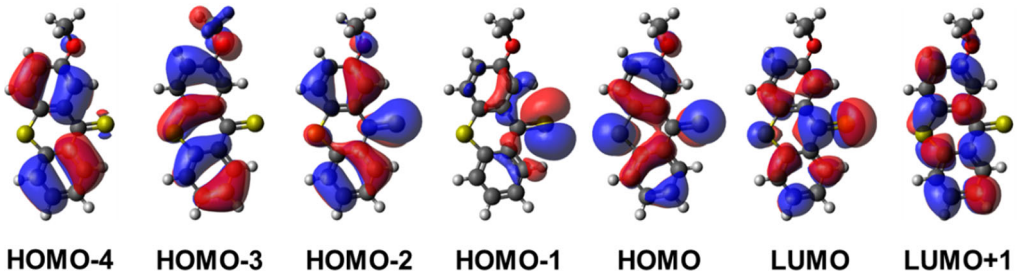

Figure S2. Molecular orbitals of **1** calculated at ωB97X-D3/def2-TZVP level.

Table S3. Energy levels and electronic transition characters of **2** optimized in the lowest singlet excited state. The frontier molecular orbitals of the dye are shown in Figure S3.

State	Energy	Oscillator strength	Transition
S_1	3.339 eV (371 nm)	0.0002	HOMO-2→LUMO (88.0%) HOMO-2→LUMO+7 (5.6%)
S_2	3.640 eV (341 nm)	0.0957	HOMO→LUMO (93.7%)
S_3	4.523 eV (274 nm)	0.0075	HOMO→LUMO+1 (40.6%) HOMO-1→LUMO (34.3%)
S_4	4.885 eV (254 nm)	0.0044	HOMO-4→LUMO (43.2%) HOMO→LUMO+1 (13.3%) HOMO→LUMO+2 (12.3%) HOMO-1→LUMO (11.3%)
S_5	4.999 eV (248 nm)	0.0504	HOMO-3→LUMO (50.8%) HOMO-1→LUMO (25.0%)
S_6	5.304 eV (234 nm)	0.8045	HOMO-4→LUMO (27.8%) HOMO→LUMO+1 (25.5%) HOMO→LUMO+4 (16.1%) HOMO-3→LUMO (10.6%)

T_1	2.486 eV (499 nm)	0	HOMO→LUMO (55.0%) HOMO-1→LUMO (15.5%) HOMO-3→LUMO (13.8%)
T_2	2.873 eV (432 nm)	0	HOMO-2→LUMO (86.6%) HOMO-2→LUMO+7 (6.6%)
T_3	3.042 eV (408 nm)	0	HOMO→LUMO (32.8%) HOMO-1→LUMO (21.4%) HOMO-3→LUMO (13.7%) HOMO-4→LUMO+2 (7.9%) HOMO→LUMO+3 (7.0%)
T_4	3.210 eV (386 nm)	0	HOMO-4→LUMO (31.4%) HOMO→LUMO+1 (21.8%) HOMO-3→LUMO+2 (9.4%) HOMO-1→LUMO (5.2%) HOMO→LUMO+2 (4.7%)
T_5	3.768 eV (329 nm)	0	HOMO-3→LUMO (22.7%) HOMO→LUMO+1 (20.1%) HOMO-1→LUMO (15.0%) HOMO→LUMO+2 (14.5%) HOMO-4→LUMO (11.4%)

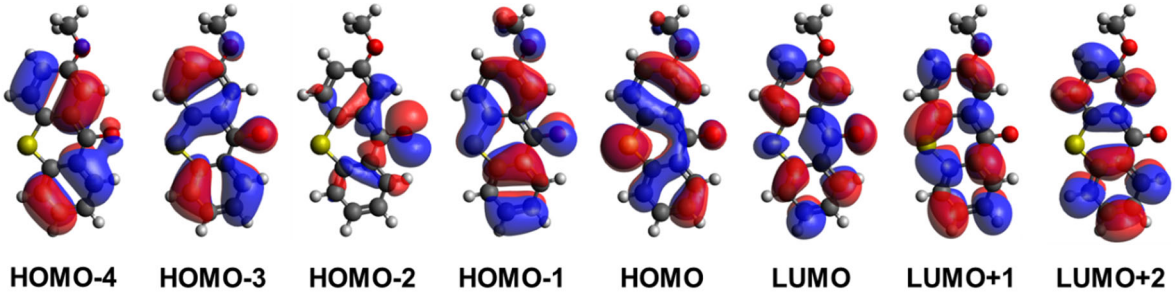

Figure S3. Molecular orbitals of **2** calculated at ωB97X-D3/def2-TZVP level.

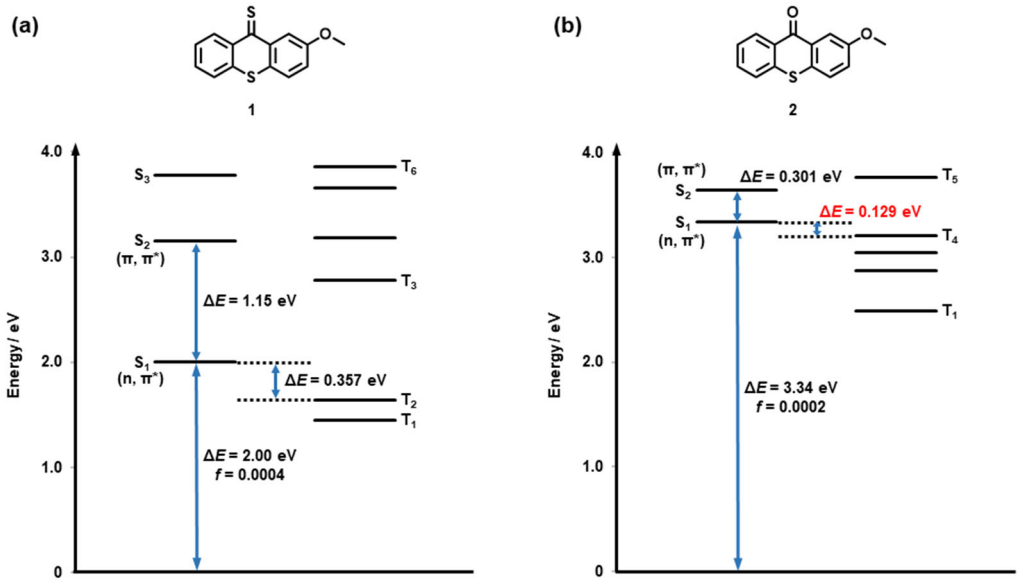

Figure S4. Energy diagrams of **1** (a) and **2** (b), optimized in the lowest singlet excited state.

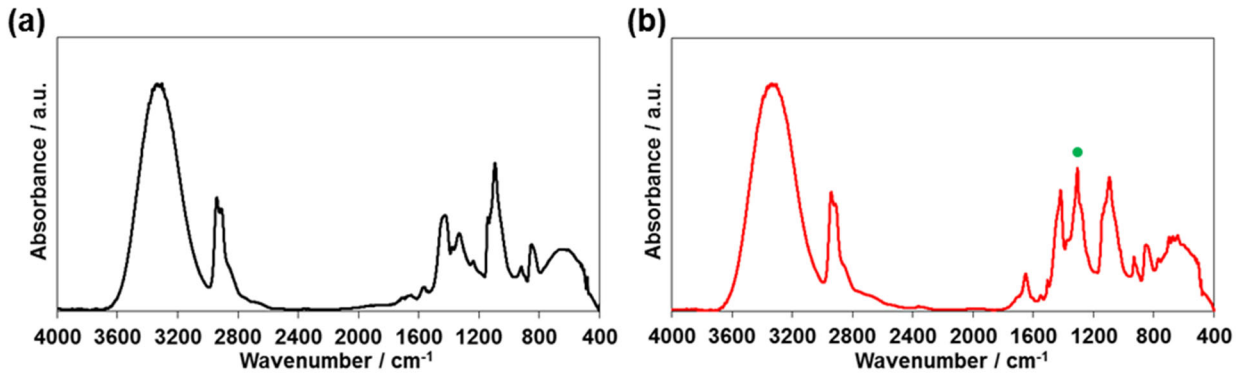

Figure S5. FT IR spectra of PVA film (a) and **BPB@PVA** (b).

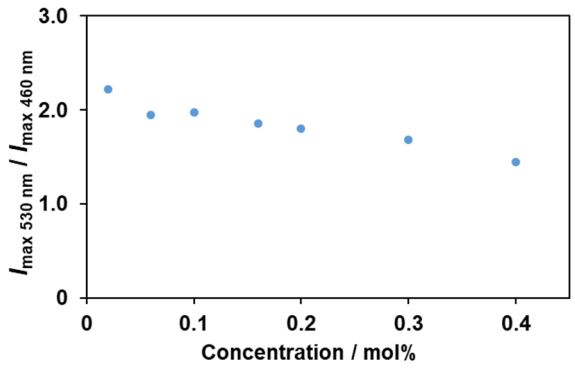

Figure S6. Change in the delayed emission intensity ratios ($I_{530\ nm}/I_{460\ nm}$) by varying concentrations of **2** doped into **BPB@PVA**. λ_{ex} = 325 nm. Delay time = 50 ms.

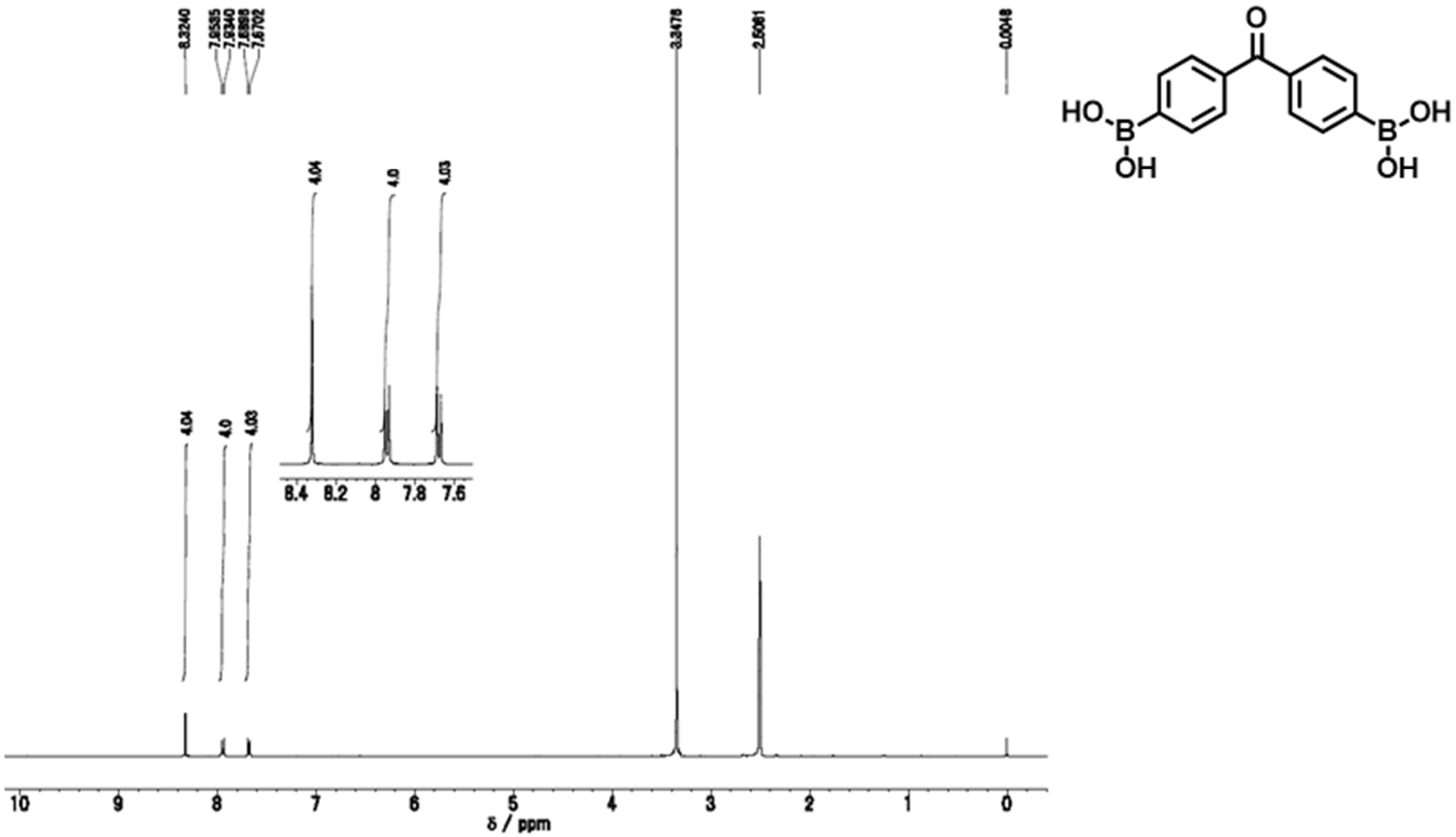

Figure S7. ^{1}H NMR spectrum (400 MHz) of **BPBA** in DMSO-d_6.

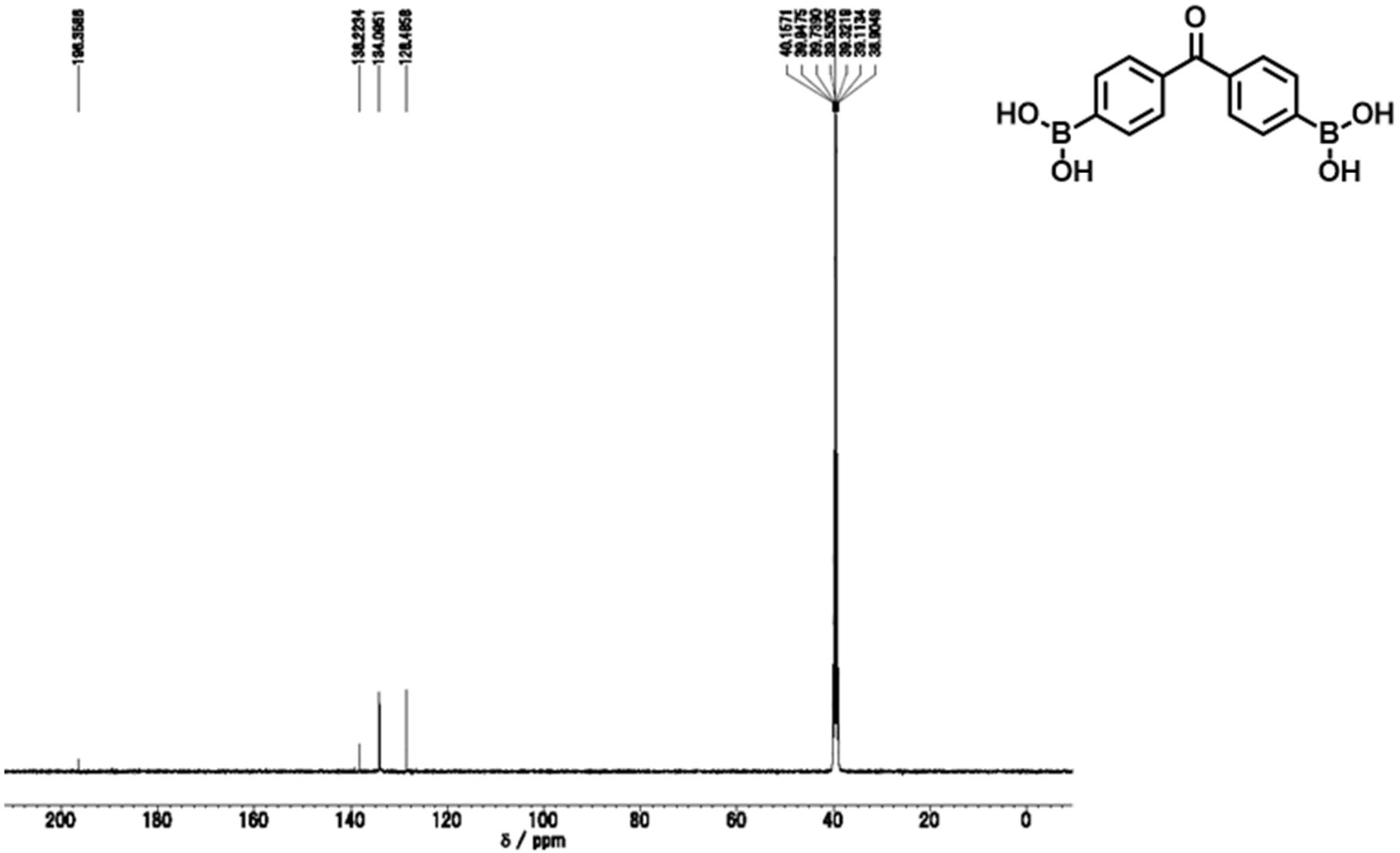

Figure S8. ^{13}C NMR spectrum (101 MHz) of **BPBA** in DMSO-d_6.

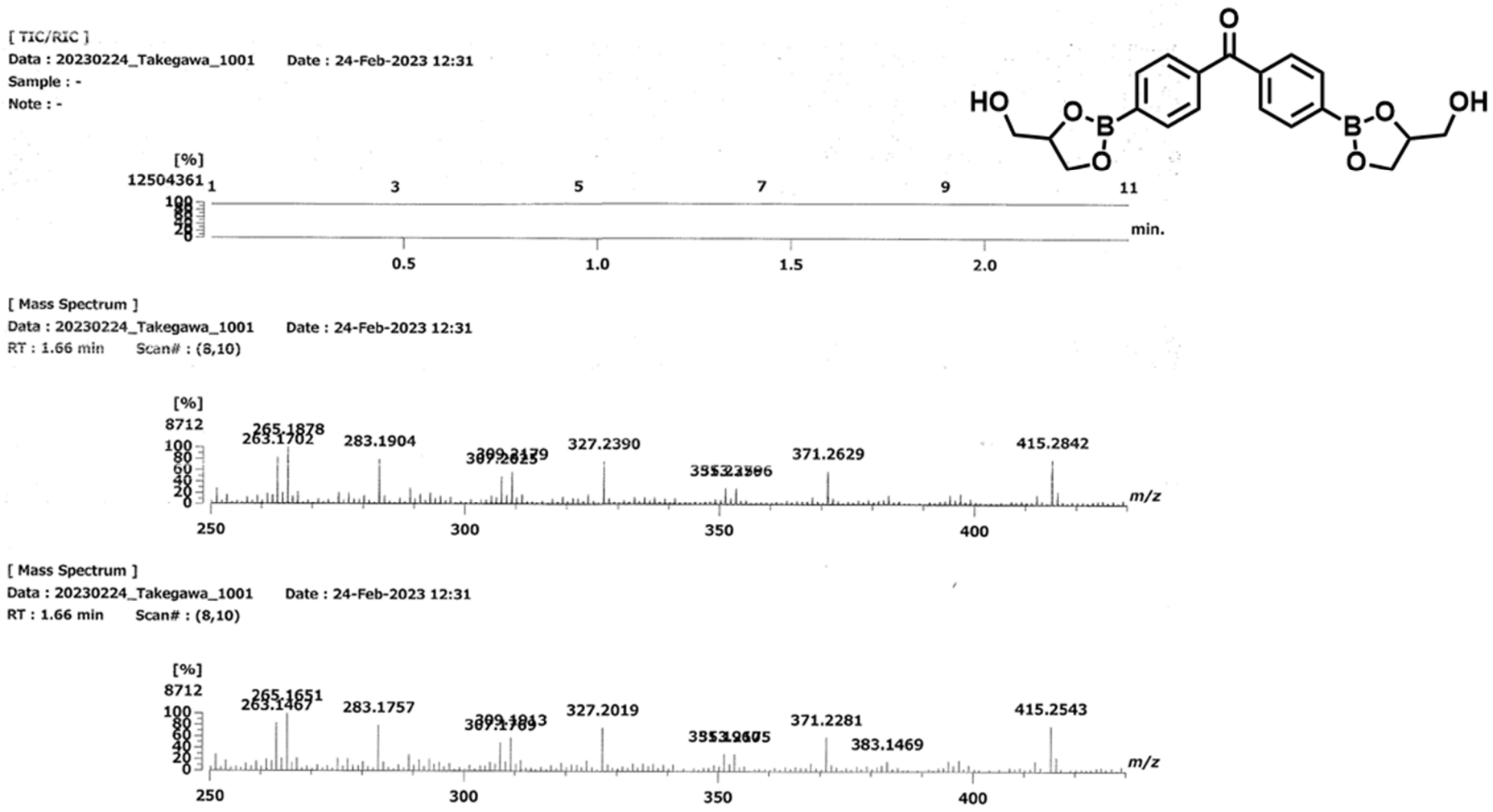

Figure S9. HR FAB-MS spectra of **BPBA**.

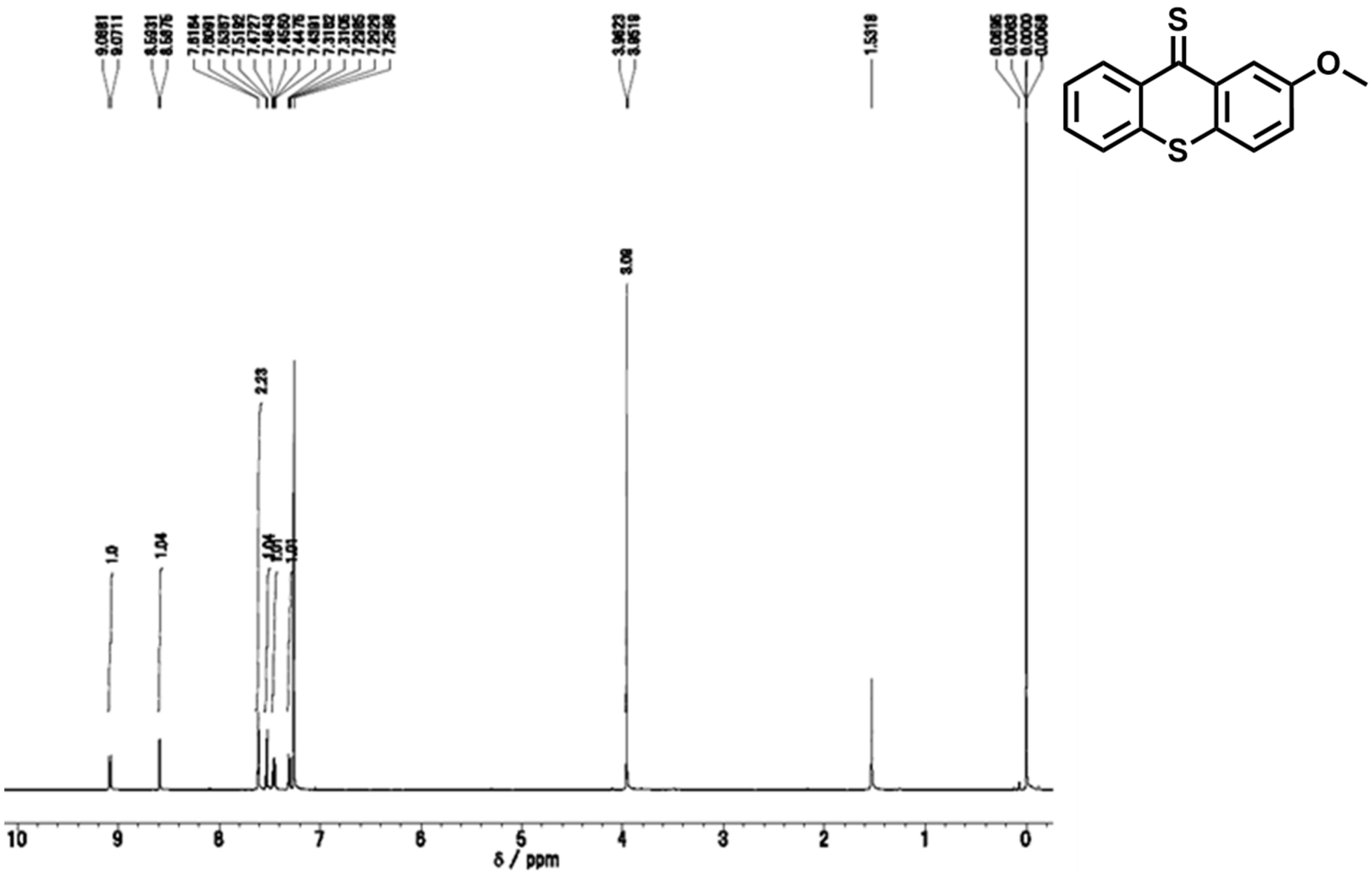

Figure S10. ^{1}H NMR spectrum (500 MHz) of **1** in $CDCl_3$.

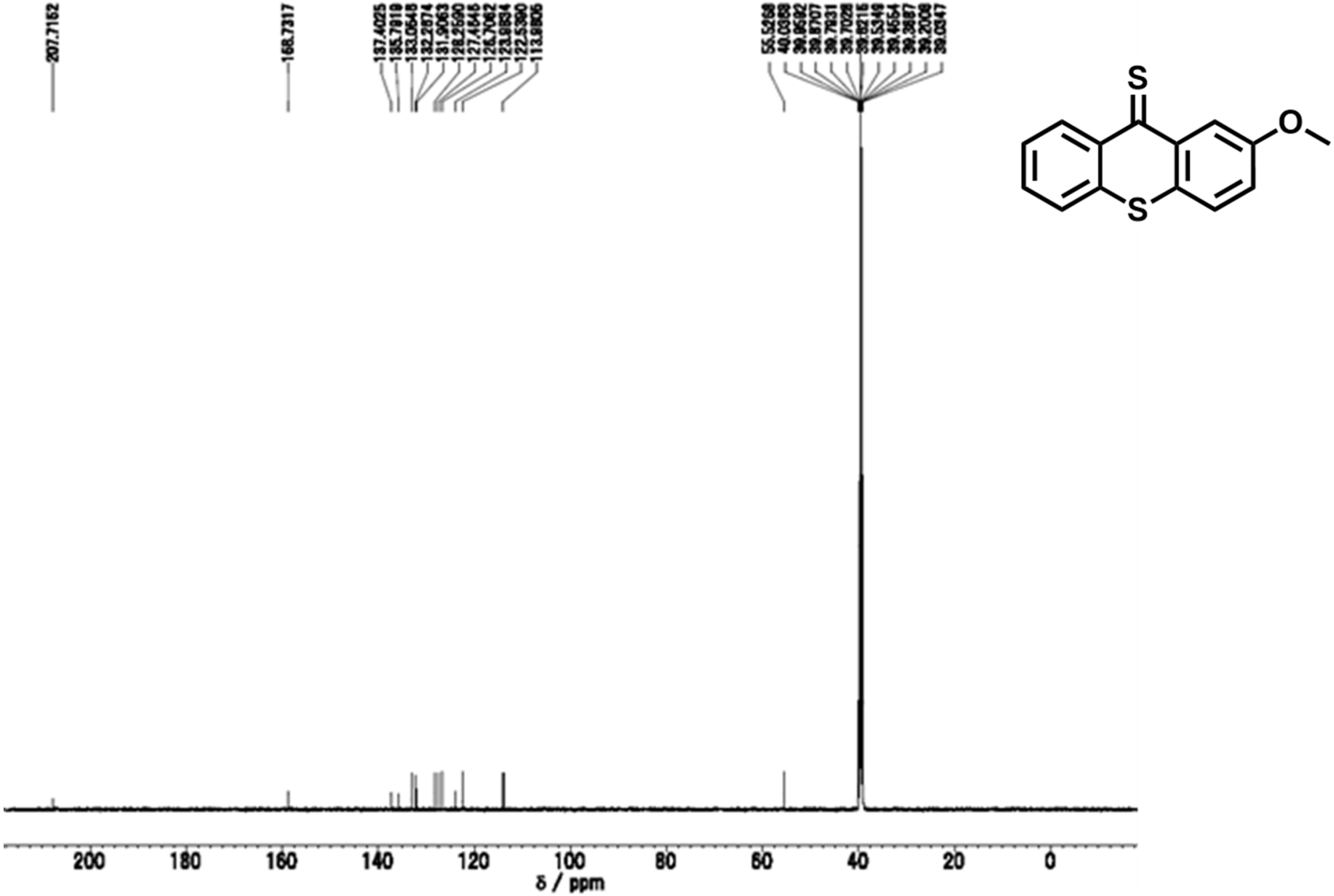

Figure S11. ^{13}C NMR spectrum (126 MHz) of **1** in DMSO-d_6.

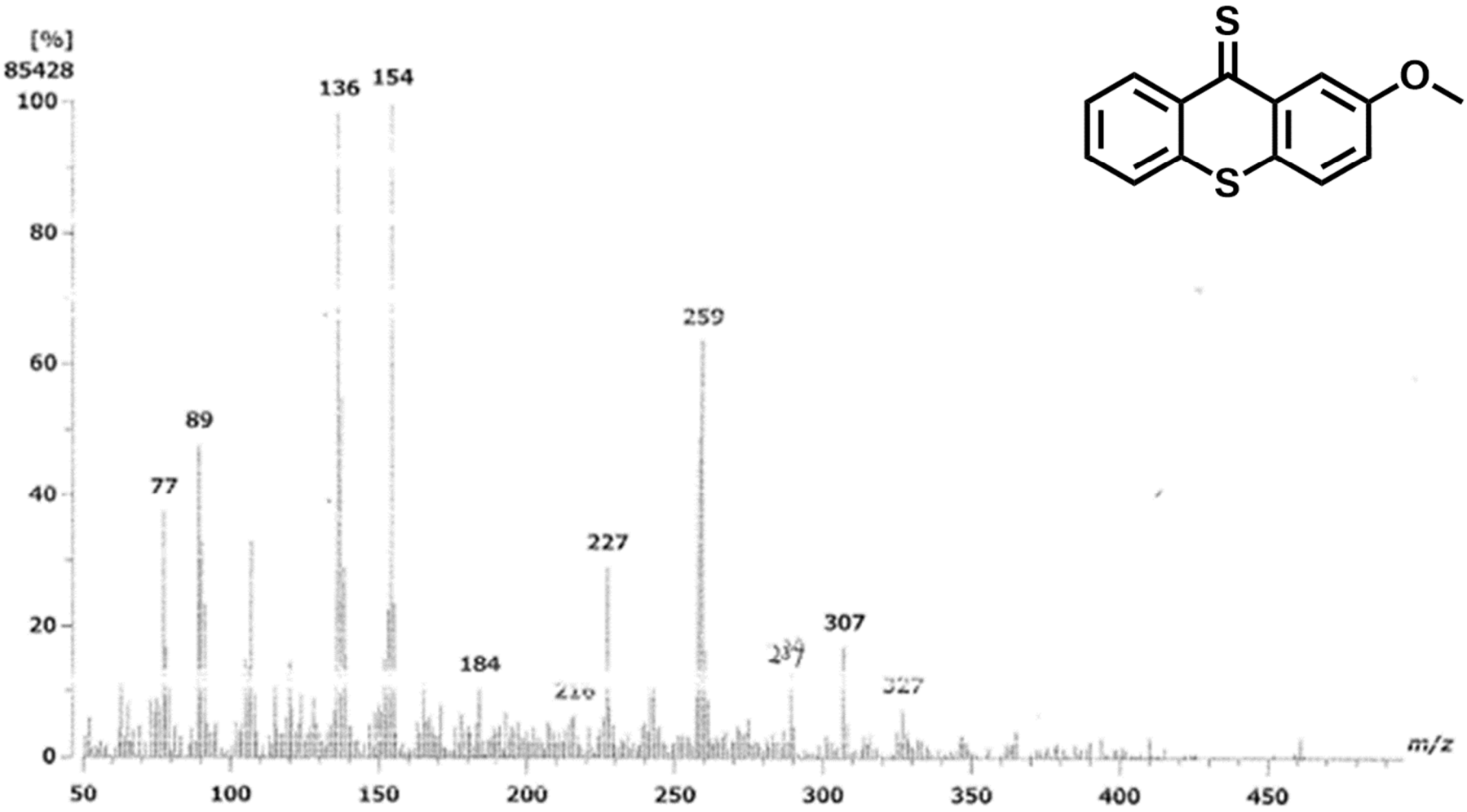

Figure S12. FAB-MS spectra of **1**.